# Radiological and histopathological features of short rib-polydactyly syndrome type III and identification of two novel *DYNC2H1* variants

CHUN-LING XIA[1*], SHI-QI XIAO[2*], XUE YANG[1], CAI-XIA LIU[1], HAO QIU[3], HONG-KUN JIANG[4], JESSE LI-LING[5] and YUAN LYU[1]

[1]Department of Gynecology and Obstetrics, Key Laboratory of Maternal-Fetal Medicine of Liaoning Province, Key Laboratory of Obstetrics and Gynecology of Higher Education of Liaoning Province, Liaoning Centre for Prenatal Diagnosis, Research Center of China Medical University Birth Cohort, Shengjing Hospital of China Medical University; [2]Department of Nursing, Shengjing Hospital of China Medical University, Shenyang, Liaoning 110004; [3]Dian Diagnostics Group Co., Ltd., Hangzhou, Zhejiang 310030; [4]Department of Pediatrics, The First Affiliated Hospital of China Medical University, Shenyang, Liaoning 110001; [5]Jinxin Research Institute of Reproductive Medicine and Genetics, Jinjiang Maternal and Children's Health Care Hospital, Chengdu, Sichuan 610041, P.R. China

Received July 31, 2020; Accepted February 18, 2021

DOI: 10.3892/mmr.2021.12065

**Abstract.** Short rib-polydactyly syndrome type III (SRPS3) is a lethal perinatal skeletal disorder consisting of polydactyly and multi-system organ abnormalities. To further assess the pathogenicity of two pairs of compound heterozygotes and to search for novel molecular etiology, X-rays and hematoxylin and eosin staining were conducted in three cases: Two retrospective samples and a newly identified patient with SRPS3. In addition, next-generation sequencing was used to evaluate a fetus with SRPS3. Typical radiological features of the three cases included a long, narrow thorax with short ribs, shortened long bones, spurs at the metaphysis of the long bones and congenital bowing of the femurs. The present study also observed atypical histopathological changes, together with the absence of proliferation and abundance of retaining cartilage in the primary spongiosum. In addition, two novel compound heterozygous variants were identified in the dynein cytoplasmic 2 heavy chain 1 (*DYNC2H1*) gene of the fetus: NM_001080463.1, c.6591_6593delTGG (chr11:103055738-103055740); NM_001080463.1, c.7883T>C (chr11:103070000). The findings of the present study provided further confirmation of the pathogenicity of two compound heterozygous variants in two retrospective samples and identified novel compound heterozygous variants. These findings may improve our knowledge of the histopathological and radiological changes in patients with SRPS3 and the relative effects of *DYNC2H1* variants. The findings of the present study may facilitate the clinical and molecular diagnosis of SRPS3.

*Correspondence to:* Dr Yuan Lyu, Department of Gynecology and Obstetrics, Key Laboratory of Maternal-Fetal Medicine of Liaoning Province, Key Laboratory of Obstetrics and Gynecology of Higher Education of Liaoning Province, Liaoning Centre for Prenatal Diagnosis, Research Center of China Medical University Birth Cohort, Shengjing Hospital of China Medical University, 36 Sanhao Street, Hepin, Shenyang, Liaoning 110004, P.R. China
E-mail: hawk.lv@163.com

*Contributed equally

*Key words:* dynein cytoplasmic 2 heavy chain 1 gene, short rib-polydactyly syndrome type III, next-generation sequencing, novel variant, histopathology

## Introduction

Short rib-polydactyly syndrome (SRPS) consists of a group of rare, genetically heterogeneous, autosomal recessive osteochondrodysplasias, which are characterized by short ribs and limbs, hypoplastic thorax, polydactyly and multisystem organ abnormalities (1). An accurate diagnosis of SRPS is difficult to obtain using prenatal ultrasound technology alone, due to overlapping phenotypic features that are characteristic of a large numbers of skeletal dysplasias (2,3). Indeed, four different types of SRPS have been identified, including SRPS1/3 (MIM 613091), SRPS2 (MIM 263520), SRPS4 (MIM 269860) and SRPS5 (MIM 614091) (4). SRPS3 is a perinatal lethal skeletal disorder, with or without polydactyly, which is characterized by a constricted thoracic cage, short ribs, shortened tubular bones and a 'trident'-like appearance of the acetabular roof.

The present study aimed to further investigate the pathogenicity of two pairs of compound heterozygotes identified in two retrospective samples and search for new molecular

etiology in a third SRPS3 fetus. The results revealed novel radiological and histopathological changes observed in the two retrospective samples (5,6). The present study also reported the case of a separate Chinese family, wherein a fetus was diagnosed with skeletal dysplasia. Targeted next-generation sequencing (NGS) panels were used to evaluate 463 known skeletal dysplasia-associated genes in both the parents and fetus. Hematoxylin and eosin (H&E) staining was also conducted. Typical and atypical histopathological features, typical radiological changes and novel dynein cytoplasmic 2 heavy chain 1 gene (*DYNC2H1*) compound heterozygous variants were identified. The findings of the present study may facilitate the clinical and molecular diagnosis of SRPS3.

## Materials and methods

*Case presentation*. Between January 2015 and December 2018, recruitment of patients and the collection of samples, from two Chinese families, were described in previous reports (5,6). The present study also included another two-generation nonconsanguineous Han Chinese family, focusing on a patient with SRPS3. The mother, a 30-year-old woman with no history of skeletal dysplasia, was referred to the Liaoning Centre for Prenatal Diagnosis (Shenyang, China) at 21 weeks of gestation because prenatal sonography had identified a fetus with short limbs and a narrow thorax (Fig. 1). Further ultrasonography revealed a normal amount of amniotic fluid, a thoracic circumference of 10.6 cm (<5th percentile), a femur length of 1.6 cm (<5th percentile) and a humerus length of 1.9 cm (<5th percentile). The biparietal diameter and head circumference of the fetus measured 4.9 and 18 cm, respectively, which was normal for the gestational age. Abnormalities were not detected in the liver and pancreas, but the kidneys were polycystic. The present study was approved by the ethics committee of Medical Scientific Research and New Technology of Shengjing Hospital of China Medical University (approval no. 2016PS159K; Shenyang, China). Informed consent was obtained for each participant included in the study.

*H&E staining*. Sections from each paraffin block of the distal femur growth plates, taken from the previously reported cases, the newly identified case and aborted fetuses without skeletal malformations were processed and stained with H&E according to routine protocols. In brief, the distal femur growth plates were fixed in 4% paraformaldehyde for 24 h at 4˚C, followed by decalcification with a decalcifying solution. Subsequently, the samples were washed in tap water for 24 h to clean the tissues, and then dehydrated in serially graded ethanol solutions and embedded in paraffin (Tissue Tek processor and Leica embedder; Leica Microsystems, Inc.). The sections (5 $\mu$m) were sagittally sectioned at a thickness of 5 $\mu$m, and deparaffinized in xylene, rehydrated in descending concentrations of alcohol, and stained with H&E (Thermo Fisher Scientific, Inc.) using routine protocols. The images were acquired under at x10 and x40 magnification using a light microscope (Nikon ECLIPSE Ci; Nikon Corporation).

*NGS and Sanger sequencing*. Peripheral blood was collected from the parents and amniotic fluid was collected from the fetus. Targeted capturing, NGS and data analysis were conducted as previously described (6). In brief, genomic DNA (case 3 I-1, I-2 and II-1) sequences were captured by a customized capture array (NimbleGen; Roche Applied Science), which was designed to capture all exons and splicing areas of 463 genes known to be associated with genetic skeletal disorders, including SRPS. The library was sequenced on an Illumina HiSeq 2000 (Illumina, Inc.). NGS produced >200 times the average sequencing depth and >98.95% overall coverage. The human reference sequence GRCh37.-hg19 was used to validate the experimental sequencing data. The pathogenicity of variants was annotated by referring to the ClinVar dataset (https://www.ncbi.nlm.nih.gov/clinvar/), Human Gene Mutation Database (http://www.hgmd.cf.ac.uk/) and the Standards and Guidelines for the Interpretation of Sequence Variants of American College of Medical Genetics and Genomics (7). Variants with minor allele frequencies (<0.01) in any of the following databases were selected: gnomAD (https://gnomad.broadinstitute.org/), Exome Aggregation Consortium (https://gnomad.broadinstitute.org/), 1000 Genomes Project (https://www.internationalgenome.org/) and an in-house database. The M-Cap tool (M-CAP version 1.4; http://bejerano.stanford.edu/MCAP/) was used to predict the variant pathogenicity. As an autosomal recessive inheritance model should be applied according to the pedigree chart, variants of compound heterozygotes or homozygotes should be relevant first. The *DYNC2H1* variants were amplified by general PCR and sequenced using two *DYNC2H1*-specific primer pairs, as follows: Primer7883 forward, 5'-GCCAATATA TTTATCCAGGATTACC-3' and Primer7883 reverse, 5'-AAA CCAAATAAAGCAAAAGAGAGTG-3'; and Primer6591_6593 forward, 5'-TGAGTTTAAAAATGGTTCTTGAAAAGG-3' and Primer6591_6593 reverse, 5'-CAAATCATTGTGTTTTGG CAGTTAAG-3'.

## Results

*Radiographic presentation of SRPS3 cases*. Radiographs of all three cases demonstrated similar skeletal characteristics, including the typical phenotypic trident appearance of the acetabulum; a long, narrow thorax with short ribs; shortened long bones; shortened femurs and remarkable spurs at the metaphysis of the long bones (Fig. 1A-C). In addition, case 3 showed obvious congenital bowing of both femurs (Fig. 1C and Table I).

*Cartilage growth plate abnormalities due to DYNC2H1 variants*. Histological sections of the distal femur growth plates obtained from the three cases were stained with H&E (Fig. 2). As shown in Fig. 2D, the growth plate of the femur bone from an aborted fetus without skeletal malformations had regular organized zones of proliferation and hypertrophy. However, in case 1, zones of proliferation and hypertrophy could not be visualized; thus, the chondrocytes did not appear to be proliferating. Within the region of osteogenesis, the primary spongiosum showed an abundance of retaining cartilage (Fig. 2A). By contrast, in cases 2 and 3, although proliferation was evident, irregular columnar formations and a lack of normal chondrocytes were observed; indeed, the chondrocytes appeared to be increasingly hypertrophic. Disorganization and

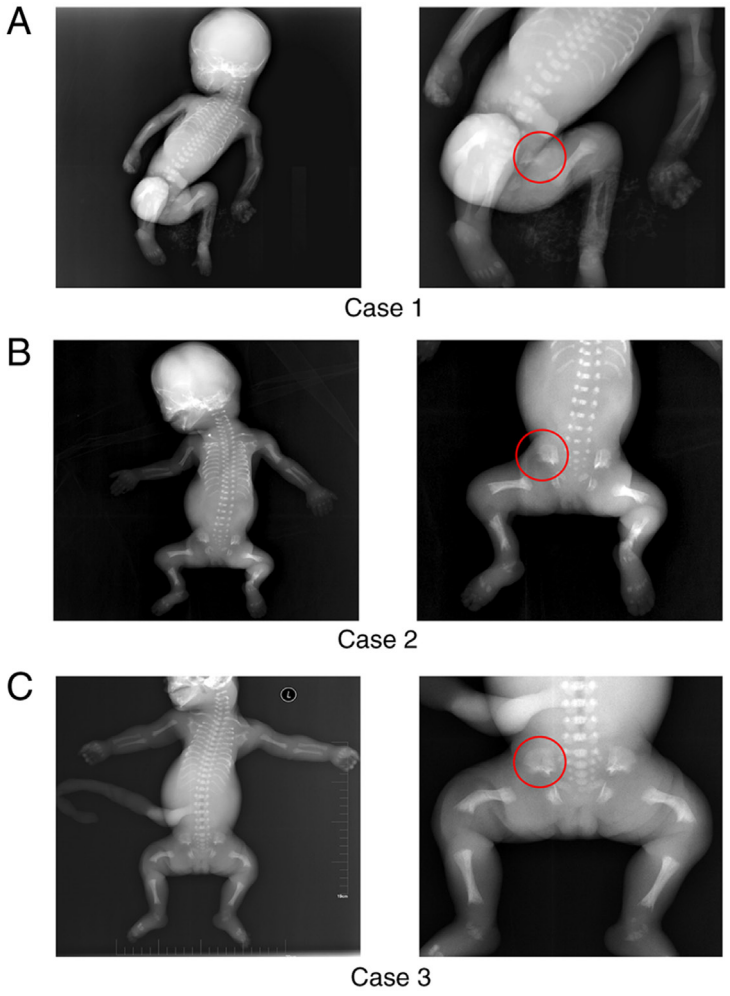


Figure 1. Radiographs of three cases of SRPS3. (A and B) Radiographs of retrospective SRPS3 samples. (C) Radiographs of the newly identified SRPS3 sample. In all three cases, we observed a trident appearance of the acetabulum (as indicated by the red ring); a long, narrow thorax with short ribs; shortened long bones; shortened femurs and remarkable spurs at the metaphysis of the long bones. Case 3 showed obvious congenital bowing of both femurs. SRPS3, short rib-polydactyly syndrome type III.

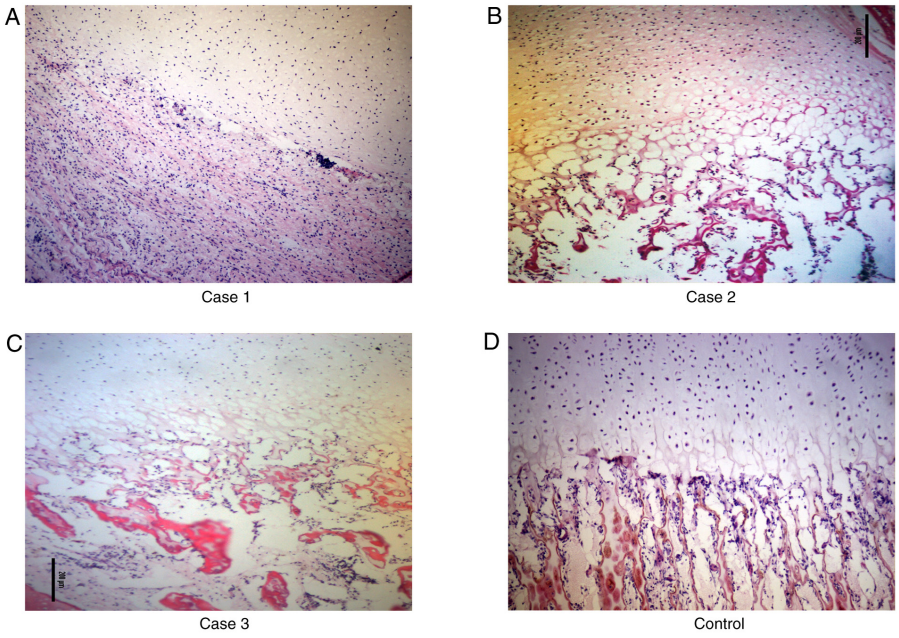


Figure 2. Photomicrographs of the femur growth plate of three cases and a control. (A) Proliferation and hypertrophy were not visualized in case 1. Primary spongiosum showed an abundance of retaining cartilage (magnification, x100). Irregular columnar formations and a lack of chondrocytes were observed in cases 2 (B) and 3 (C) (magnification, x200). Disorganization and increased vacuolization were evident in the region of osteogenesis. (D) Regularly organized zones of proliferation and hypertrophy were seen in the growth plate of a femur bone from an unaffected control fetus (magnification, x200).

Table I. Clinical features of cases with SRPS3.

| | Cases | | |
|---|---|---|---|
| Clinical features | Case 1 | Case 2 | Case 3 |
| CS | No | No | No |
| Week of diagnosis, wg | 25 | 28 | 21 |
| Diagnosis | SRPS3 | SRPS3 | SRPS3 |
| Chest circumference, cm | NA | 11.2 | 10.6 |
| Abdominal circumference, cm | 19.9 | 13.8 | 14.4 |
| Femur length, cm | 3.4 | 2.1 | 1.6 |
| Humerus length, cm | 3 | 2.1 | 1.9 |
| Polydactyly | No | No | No |
| Kidney anomaly | No | No | Polycystic kidney |
| Liver/pancreas microscopic changes | No | No | No |
| Trident appearance of acetabulum | Yes | Yes | Yes |
| Short ribs | Yes | Yes | Yes |
| Short long bones | Yes | Yes | Yes |
| Long bones, metaphysis spurs | Yes | Yes | Yes |
| Congenitally bowed femurs | No | No | Yes |
| Histopathological changes | Irregularly organized proliferation and hypertrophy zones | Irregularly organized proliferation and hypertrophy zones | NA |
| Other features | NA | NA | NA |

SRPS3, short rib-polydactyly syndrome type III; CS, consanguinity; wg, weeks of gestation; NA, not available.

increased vacuolization were evident in the region of osteogenesis (Fig. 2B and C).

*Novel variants identified in SRPS3 case 3*. Targeted exon sequencing of 463 known skeletal disorder-related genes was performed in the newly identified proband and parents (case 3, Fig. 3A-3). Together, two compound heterozygous maternal and paternal variants were identified in the *DYNC2H1* gene: NM_001080463.1, c.6591_6593delTGG (chr11:103055738-103055740) and NM_001080463.1, c.7883T>C (chr11:103070000), respectively. These results were further confirmed by Sanger sequencing. The two variants were highly conserved upon comparison of the sequences over a range of species (Fig. 3B).

## Discussion

All three fetuses considered in this report showed prenatal sonographic findings that were consistent with SRPS and all parents agreed to induced labor. Radiography showed similar phenotypes for the three fetuses (Fig. 1). These findings were consistent with previous reports regarding the radiographic presentation of SRPS3 cases (5,6). Although other multisystem anomalies are often associated with SRPS (8), only a polycystic kidney was found in case 3 (Table I).

A number of histopathological changes have been found in the growth plates of patients with SRPS. Such phenomena have been observed in several skeletal dysplasia-associated genes, including intraflagellar transport protein 43 homolog (*IFT43*), *IFT80* and *IFT52* (9-11). However, few histopathological changes have been reported in the growth plates of cases involving *DYNC2H1* variant-induced SRPS (7). To confirm the involvement of *DYNC2H1* variants in endochondral ossification, the histological sections of femur growth plates were stained. Case 1 was atypical, wherein proliferation was absent and an abundance of retaining cartilage was observed in the primary spongiosum (Fig. 2A). Phenotypes similar to those reported in the literature were observed in cases 2 and 3 (Fig. 2B and C).

Variants in *DYNC2H1* can inactivate the retrograde ciliary motor, causing skeletal dysplasia (12). A number of the morphological abnormalities observed in human ciliopathies are probably caused by disruption of the hedgehog signaling pathway, including variation in the *DYNC2H1* gene (13,14). Although different histopathological changes were observed in the three cases evaluated in the present study, they all showed an abnormal pattern of proliferation and differentiation at the femur growth plates. This may be due to disruption of the hedgehog signaling pathway caused by a *DYNC2H1* variant.

One of the novel *DYNC2H1* variants found in case 3 (Fig. 3A-3), namely c.7883T>C(p.Leu2628Ser) (chr11:103070000), is located in exon 49 within an ATP binding and hydrolysis domain (AAA_4 domain). The M-Cap tool predicted this variant to be 'deleterious'. Regardless of this prediction, this variant occurs in the conserved AAA_4 domain, which should affect ATP binding and hydrolysis. In addition, another variant, reported to cause SRPS, has been located within close proximity to c.7883T>C (15).

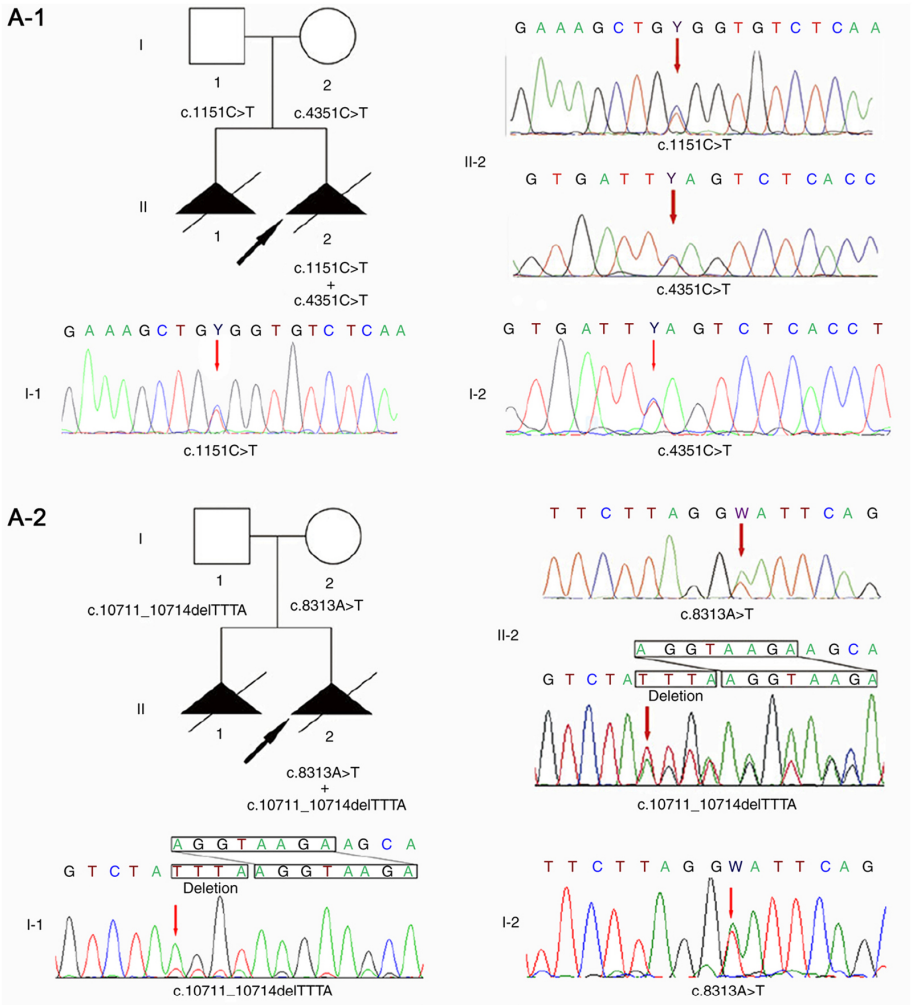


B

Gly2198del

| Species | aa | Alignment |
|---|---|---|
| Human | 2197 | DEFIINLIRGLGGNLNMKSRLEFT |
| Mutated | 2197 | DEFIINLIRGL-GNLNMKSRLEF |
| Ptroglodytes | 2195 | DEFIINLIRGLGGNL NMKSRLEF |
| Mmusculus | 2197 | DQFIINLIRGLGGNLNMKSRLEF |
| Ggallus | 2195 | GQFIINLLRGLGGNLNMSSRLEF |
| Trubripes | 2196 | GQFIIGLLRGLGGNINFKTRQEF |

Leu2628Ser

| Species | aa | Alignment |
|---|---|---|
| Human | 2628 | HYGRDNQNLDILLFHEVLEYMSRI |
| Mutated | 2628 | HYGRDNQNLDISLFHEVLEYMSR |
| Ptroglodytes | 2626 | HYGRDNQNLDILLFHEVLEYI SR |
| Mmulatta | 46 | HYGRDNQNLDILLFHEVLEYMSR |
| Mmusculus | 2628 | HYGRDNQNLDILLFQEVLEYMSR |
| Ggallus | 2625 | HYGRDKKEIEILLFQEVLNY V SR |
| Trubripes | 2626 | LYSRDNRELDILLFREV |

Figure 3. *DYNC2H1* variants identified in three short rib-polydactyly syndrome type III families. (A) Pedigree and variants identified in three cases, (A-1) case 1, (A-2) case 2 and (A-3) case 3. (B) Conservation of *DYNC2H1* residues. The identified mutant amino acids were highly conserved between different species. *DYNC2H1*, dynein cytoplasmic 2 heavy chain 1 gene.

The other variant identified in this study in case 3, c.6591_6593delTGG(Gly2198del) (chr11:103055738-103055740; Fig. 3A-3), might hinder ATP hydrolysis and thus, the generation of adequate cellular energy for the movement of microtubules. An R2205H substitution close to the novel variant has also been reported to cause SRPS (16). Neither p.Leu2628Ser nor Gly2198del were detected in the control database, indicating that these two variants were pathogenic in nature, rather than polymorphisms.

The present study identified atypical histopathological changes and confirmed the radiological features of three SRPS3 cases. In addition, it successfully diagnosed SRPS3 in a Chinese fetus and identified two novel compound heterozygous *DYNC2H1* variants. In conclusion, three pairs of compound heterozygous *DYNC2H1* variants were identified as pathogenic. The findings of the present study expand the current understanding of histopathological changes associated with *DYNC2H1* variants and provide further confirmation of the radiological features of SRPS3. Collectively, the findings should promote more efficient imaging, as well as histopathological and molecular diagnoses of SRPS3.

**Acknowledgements**

Not applicable.

**Funding**

The present study was jointly supported by the Natural Science Foundation of China (grant no. 81701462), the National Key R&D Program of China (grant no. 2018YFC1002900) and the 345 Talent Project.

**Availability of data and materials**

The datasets generated and/or analyzed during the current study are not publicly available due to the participants not wanting to share all their sequencing data on a public database except for the pathogenic variants, but are available from the corresponding author on reasonable request.

**Authors' contributions**

CLX, SQX, XY and YL conceived and designed the experiments. CXL, HKJ, JLL and YL assisted in the recruitment of the patients and acquisition of experimental data. CLX, SQX, XY and HQ performed the experiments. SQX , XY, YL and HQ helped in genetic analysis. CLX , SQX , XY, YL and HQ wrote the manuscript. CLX and YL confirm the authenticity of all the raw data. All authors read and approved the final manuscript.

**Ethics approval and consent to participate**

All procedures performed in studies involving human participants were in accordance with the ethical standards of the institutional and/or national research committee and in accordance with the 1964 Helsinki declaration and its later amendments or comparable ethical standards. This study was approved by the ethics committee of Medical Scientific Research and New Technology of Shengjing Hospital of China Medical University (approval no. 2016PS159K; Shenyang, China). Informed consent was obtained for each participant included in the study.

**Patient consent for publication**

Not applicable.

**Competing interests**

The authors declare that they have no competing interests.

**References**

1. Huber C and Cormier-Daire V: Ciliary disorder of the skeleton. Am J Med Genet C Semin Med Genet 160C: 165-174, 2012.
2. Krakow D and Rimoin DL: The skeletal dysplasias. Genet Med 12: 327-341, 2010.
3. Mäkitie O: Molecular defects causing skeletal dysplasias. Endocr Dev 21: 78-84, 2011.
4. Bonafe L, Cormier-Daire V, Hall C, Lachman R, Mortier G, Mundlos S, Nishimura G, Sangiorgi L, Savarirayan R, Sillence D, *et al*: Nosology and classification of genetic skeletal disorders: 2015 revision. Am J Med Genet A 167A: A2869-A2892, 2015.
5. Chen LS, Shi SJ, Zou PS, Ma M, Chen XH and Cao DH: Identification of novel DYNC2H1 mutations associated with short rib-polydactyly syndrome type III using next-generation panel sequencing. Genetics and molecular research. Genet Mol Med 15: gmr8134, 2016.
6. Mei L, Huang Y, Pan Q, Su W, Quan Y, Liang D and Wu L: Targeted next-generation sequencing identifies novel compound heterozygous mutations of DYNC2H1 in a fetus with short rib-polydactyly syndrome, type III. Clin Chim Acta 447: 47-51, 2015.
7. Richards S, Aziz N, Bale S, Bick D, Das S, Gastier-Foster J, Grody WW, Hegde M, Lyon E, Spector E, *et al*; ACMG Laboratory Quality Assurance Committee: Standards and guidelines for the interpretation of sequence variants: A joint consensus recommendation of the American College of Medical Genetics and Genomics and the Association for Molecular Pathology. Genet Med 17: 405-424, 2015.
8. Elçioglu NH and Hall CM: Diagnostic dilemmas in the short rib-polydactyly syndrome group. Am J Med Genet 111: 392-400, 2002.
9. Zhang W, Taylor SP, Nevarez L, Lachman RS, Nickerson DA, Bamshad M, Krakow D and Cohn DH; University of Washington Center for Mendelian Genomics Consortium: IFT52 mutations destabilize anterograde complex assembly, disrupt ciliogenesis and result in short rib polydactyly syndrome. Hum Mol Genet 25: 4012-4020, 2016.
10. Cavalcanti DP, Huber C, Sang KH, Baujat G, Collins F, Delezoide AL, Dagoneau N, Le Merrer M, Martinovic J, Mello MF, *et al*: Mutation in IFT80 in a fetus with the phenotype of Verma-Naumoff provides molecular evidence for Jeune-Verma-Naumoff dysplasia spectrum. J Med Genet 48: 88-92, 2011.
11. Duran I, Taylor SP, Zhang W, Martin J, Qureshi F, Jacques SM, Wallerstein R, Lachman RS, Nickerson DA, Bamshad M, *et al*: Mutations in IFT-A satellite core component genes IFT43and IFT121 produce short rib polydactyly syndrome with distinctive campomelia. Cilia 6: 7, 2017.
12. Ocbina PJ, Eggenschwiler JT, Moskowitz I and Anderson KV: Complex interactions between genes controlling trafficking in primary cilia. Nat Genet 43: 547-553, 2011.
13. Weatherbee SD, Niswander LA and Anderson KV: A mouse model for Meckel syndrome reveals Mks1 is required for ciliogenesis and Hedgehog signaling. Hum Mol Genet 18: 4565-4575, 2009.
14. Goetz SC and Anderson KV: The primary cilium: A signalling centre during vertebrate development. Nat Rev Genet 11: 331-344, 2010.
15. El Hokayem J, Huber C, Couvé A, Aziza J, Baujat G, Bouvier R, Cavalcanti DP, Collins FA, Cordier MP, Delezoide AL, *et al*: NEK1 and DYNC2H1 are both involved in short rib polydactyly Majewski type but not in Beemer Langer cases. J Med Genet 49: 227-233, 2012.
16. Merrill AE, Merriman B, Farrington-Rock C, Camacho N, Sebald ET, Funari VA, Schibler MJ, Firestein MH, Cohn ZA, Priore MA, *et al*: Ciliary abnormalities due to defects in the retrograde transport protein DYNC2H1 in short-rib polydactyly syndrome. Am J Hum Genet 84: 542-549, 2009.